scientific reports

Check for updates

OPEN

Effects of different anesthetic drugs on electroretinography in mice

Chaofeng Yu[1,2], Xue Wang[3], Kunhuan Yang[4], Yun Han[4], Shiying Li[4,5] & Yi Wang[1,2]

Electrophysiology (ERG) is widely used for retinal function assessment, but the effects of different anesthetics on ERG recordings, particularly in degenerated retinas, remain unclear. This study investigated the effects of different anesthetic drugs on ERG in wild-type (WT), Kv8.2 knockout (KO), and rd10 mice. Anesthetic drugs, avertin (300 mg/kg) and pentobarbital sodium (50 mg/kg) were administered intraperitoneally, isoflurane was given at 5% for induction and 1.5% for maintenance. Full-field flash electroretinography (ff-ERG) was recorded, including scotopic and photopic responses. Specifically, the amplitudes of a-wave, b-wave, oscillatory potentials (OPs), photopic negative response (PhNR), and c-wave were analyzed, respectively. Additionally, fundus imaging and optical coherence tomography (OCT) were performed to analyze retinal morphology. The three anesthetics had no obvious effect on retinal morphology. Pentobarbital sodium decreased scotopic OPs, increased scotopic and photopic b-wave amplitudes and decreased photopic a-wave amplitude in all groups of mice. Isoflurane resulted in larger scotopic OPs and photopic a-wave amplitudes in all groups, with a larger scotopic a-wave amplitude in KO mice. The PhNR amplitude was greater in WT mice anesthetized with avertin. The ERG amplitudes in mice showed significant differences among the three anesthetic conditions. Pentobarbital sodium markedly suppressed retinal OPs, suggesting it may not be suitable for assessing inner retinal function, particularly amacrine cells. Isoflurane enabled excellent recordings of various types of ERG, making it suitable for nearly all ERG recordings. Avertin might serve as a suitable alternative in the absence of isoflurane.

Keywords Avertin, Isoflurane, Pentobarbital sodium, ERG, Kv8.2 KO, rd10

Electroretinography (ERG) provides a non-invasive, objective evaluation of retinal function. Full-field flash electroretinogram (ff-ERG) is used to record the electrical responses of various retinal neurons to light stimuli[1]. The ff-ERGs include a-wave, b-wave, c-wave, photopic negative responses (PhNR), and oscillatory potentials (OPs). Specifically, a-wave originates from photoreceptors[2,3], b-wave from bipolar and Müller cells[4,5], and c-wave from the retinal pigment epithelium (RPE)[6]. In addition, PhNR presents ganglion cell activity[7]. Meanwhile, OPs are a series of high-frequency wavelets superimposed on the rising phase of b-wave, which are related to inner retinal activity, especially that of amacrine cells[8].

ERG is more sensitive for diagnosing early retinal hereditary diseases compared with visible fundus abnormalities. In this study, wild-type (WT) mice, Kv8.2 knockout (KO) mice, and rd10 mice were used as the research subjects. Kv8.2 KO mice have been used to study retinal degeneration characterized by abnormal voltage-gated potassium channels[9]. These mice exhibited supernormal b-waves in ERG, indicating disrupted signal transmission from photoreceptors to bipolar cells[9–11]. Moreover, rd10 mice, with a mutation in the *Pde6b* gene of rod cells, have been widely used to study retinitis pigmentosa, exhibiting progressive photoreceptor degeneration, characterized by significant reductions in a- and b-wave amplitudes[12–14].

Anesthesia played a crucial role in the process of ERG recording in animal models. The combination of ketamine and xylazine is commonly used in laboratory rodents[15–18]. Ketamine, a dissociative anesthetic, is frequently used for anesthesia induction and maintenance as well as for the treatment of depression and pain.

[1]Aier Academy of Ophthalmology, Central South University, Changsha 410000, China. [2]Department of Ophthalmology, Chongqing Aier Eye Hospital, Chongqing 400020, China. [3]Department of Ophthalmology, The Second Affiliated Hospital of Anhui Medical University, Hefei 230061, China. [4]Fujian Provincial Key Laboratory of Ophthalmology and Visual Science, Fujian Engineering and Research Center of Eye Regenerative Medicine, School of Medicine, Eye Institute of Xiamen University, Xiamen University, Xiamen 361102, China. [5]Department of Ophthalmology, School of Medicine, The First Affiliated Hospital of Xiamen University, Xiamen 361003, China. ✉email: shiying_li@126.com; wangyieye@aliyun.com

However, due to its hallucinogenic and addictive properties, ketamine is classified as a controlled substance in many countries, making it less accessible for laboratory use[19–21]. Anesthetic drugs like isoflurane[22–25], avertin, and pentobarbital sodium are widely used in the experimental settings[26–28]. Isoflurane, an inhalational anesthetic, is well known for its rapid onset and fast recovery. Additionally, isoflurane helps to maintain stable physiological function, including heart rate, blood oxygen partial pressure, and blood pH levels. Therefore, it is suitable for maintaining stable retinal blood flow and retinal function in long-term experiments[29–31]. Similarly, avertin, a non-pharmaceutical-grade anesthetic, has been extensively used for various experimental manipulations in laboratory rodents due to its ready availability, lack of drug regulation, and rapid anesthetic induction and recovery time[32,33]. Pentobarbital sodium, another intraperitoneal anesthetic, has been shown to provide consistent anesthetic depth with minimal adverse effects on ERG recording, although it may suppress certain components like the scotopic threshold response (STR)[34,35].

Up to now, rare studies have systematically compared the effects of these three anesthetics on ERG recordings. Most prior research has primarily focused on wild-type mice[36–38]. Accordingly, in this study, we aimed to examine the effect of these anesthetics on ERG recordings in WT mice with healthy retinas as well as in Kv8.2 KO and rd10 mice with retinal degeneration. The results provide theoretical support for the selection of anesthetics in ERG recordings.

Methods
Animals
WT C57BL/6 J mice (male, 7–8 weeks old, 20–25 g) were purchased from Charles River Laboratories, while rd10 mice (C57BL/6 J, male, 4 weeks old, 9–11 g) were provided by Professor Zhang Zuoming from the Air Force Medical University. $KCNV2^{-/-}$ mice (C57BL/6 J) were obtained by breeding $KCNV2^{-/-}$ mice (C57BL/6N) obtained from Cyagen Bioscience Inc. (Suzhou, China) with C57BL/6 J mice for five generations, followed by self-crossing. These mice are referred to as Kv8.2 KO in this paper and were used for experiments in this study (male, 7–8 weeks old, 20–25 g). All mice were maintained under specific-pathogen-free (SPF) conditions in the Experimental Animal Center of Xiamen University, under a standard 12/12-h light/dark cycle in climate-controlled facilities, with free access to food and water. All experiments adhered to the ARRIVE guidelines for animal use in ophthalmic and vision research and the American Veterinary Medical Association (AVMA) Guidelines for the Euthanasia of Animals (2020). All methods were performed in accordance with the relevant guidelines and regulations. The study was approved by the Animal Ethics Committee of Xiamen University (approval No: XMULAC20230124).

Reagents
1.5% Isoflurane Anesthesia: An appropriate amount of isoflurane (R510-22–10, RWD) was added into the small animal anesthesia machine (R5835, RWD), and the air pump was turned on with a flow rate of 0.6L/min. Mice were placed in the induction box for anesthesia induction with isoflurane at a concentration of 5% for 2–3 min. Anesthesia was maintained with a mask at an isoflurane concentration of 1.5%.

1.25% Avertin Anesthesia: First, 10 g of avertin (T48402-25G, SIGMA) was mixed with 10 mL of tertiary amyl alcohol (R017959-100 ml, RHAWN), shaken well, and left at room temperature for 2 h to obtain a 100% stock solution of avertin. Then, 1.25 mL of the stock solution was diluted with 98.75 mL of normal saline to obtain a 1.25% concentration of avertin, which was administered intraperitoneally to mice at a dose of 300 mg/kg.

1% Pentobarbital Sodium Anesthesia: A total of 1 g of sodium pentobarbital (Merck) was dissolved in 100 mL of normal saline to obtain a 1% solution, which was then administered intraperitoneally to mice at a dose of 50 mg/kg.

Standardized anesthesia and euthanasia
The administration of the three anesthetics was performed as described above, with each mouse receiving only one type of anesthetic throughout the entire examination. Regardless of the anesthetic used, it was essential to ensure that the mouse remained still, with stable respiration and heart rate, and without obvious pain, while also maximizing the protrusion of the eyes after anesthesia—crucial for ERG recording. After completing all examinations, mice were euthanized by cervical dislocation.

Electroretinography
ERG was recorded using the RetiMINER System (AiErXi Medical Equipment Co., Ltd., Chongqing, China)[39]. After overnight dark adaptation (> 12 h), mice were anesthetized with avertin, isoflurane, or sodium pentobarbital. Their pupils were fully dilated with 0.5% tropicamide and 0.5% phenylephrine hydrochloride (SANTEN), and the corneas were coated with 0.2% carbomer gel (Bausch & Lomb) to maintain moisture and conductivity. The ground electrode was placed at the tail end, the reference electrode subcutaneously at the midline between the ears, and the gold ring electrode at the corneal apex. ERG was recorded once the oscilloscope showed stable readings, with all procedures conducted under dim red light. The heating pad integrated into the RetiMINER system remains on during the recording process to maintain the mouse's body temperature.

Scotopic ERG involved an series of single white flashes of intensity ranging from 0.001 to 30 cd s/m², with stimulus intervals increasing from 5 s to 1 min. Each stimulus intensity was recorded three times, and the waveforms were averaged using a band-pass filter of 0.3–300 Hz. OPs were recorded using dark-adapted ERG at a stimulus light intensity of 3 cd s/m², averaging three waveforms with a band-pass filter of 75–300 Hz. C-wave ERG recordings were made after a 100 ms white light stimulus at an intensity of 150 cd/m², with 1 min intervals, averaging three waveforms. Mice were light adapted for 10 min with a background light of 30 cd/m² before performing light-adapted ERG recording. After 10 min of light adaptation with a white background

light of 30 cd/m^2, photopic ERG recordings began with single white flashes ranging from 1 to 30 cd s/m^2 on a white background of 30 cd/m^2. Twenty waveforms were recorded per stimulus intensity, and they were averaged using a band-pass filter of 0.3–300 Hz. The PhNR was recorded at a stimulus intensity of 20 cd s/m^2 on a green background of 40 cd/m^2, averaging 100 waveforms with a band-pass filter of 0.3–300 Hz. After recording, the mice were placed on an electric blanket until they regained consciousness[40].

All signal recordings began 20 ms before the flash. The negative wave following the flash was designated as the a-wave, and the subsequent positive wave was designated as the b-wave. The positive wave following the b-wave was identified as the c-wave. The a-wave peak time was measured from the flash to the a-wave trough, and the b-wave peak time was measured from the flash to the b-wave peak. The a-wave amplitude was determined as the voltage difference from the baseline to the a-wave trough, and the b-wave amplitude was measured from the b-wave peak to the a-wave trough[6]. The c-wave amplitude was measured from the c-wave peak to the baseline. The OP amplitude was calculated as the sum of the three largest wavelets (OP1, OP2, OP3). The PhNR wave was identified as the largest negative wave following the b-wave in the photopic ERG, and its amplitude was the voltage difference from the peak of the b-wave to the trough of the PhNR wave. If there were significant interference signals, band-stop filtering was applied. Waveform data files were exported, and various waveform graphs were plotted using ORIGIN 2024b (OriginLab Corporation, USA).

Fundus imaging

Fundus images were collected using the OPTO-RIS small animal retinal imaging system (Optoprobe, UK). Each mouse was anesthetized with the same dose and method of the anesthetic used during its ERG recording. Their pupils were fully dilated using 0.5% tropicamide and 0.5% phenylephrine hydrochloride (SANTEN), while corneas was kept moist with 0.2% carbomer gel (Bausch & Lomb). The mice were placed on a lifting platform, and the illumination intensity and eye position were adjusted to center the optic nerve in the field of view and ensure clear imaging. After the collection, the mice were transferred to the OCT platform.

Optical coherence tomography

OCT was performed using the 4D-ISOCT super-microscopic imaging system (Optoprobe, UK). To avoid repeated anesthesia and mydriasis in mice, OCT was performed together with fundus imaging. After completing fundus imaging, the mice were transferred to the OCT platform, and their position and angle were adjusted to clearly display the retina with the optic nerve centered. The platform was moved back and forth to position the retinal cross-sectional imaging within the visible window for clearer retinal layering. After collection, the mice were placed on an electric heating pad until they regained consciousness.

Statistical analysis

All data were analyzed using GraphPad Prism 9.4 software (GraphPad Prism Software, Inc., USA) and presented as mean ± SEM. The results were analyzed using a two-way ANOVA with Geisser–Greenhouse correction followed by Tukey multiple comparisons correction. A p-value of less than 0.05 was considered to be statistically significant ($^*p < 0.05$, $^{**}p < 0.01$, $^{***}p < 0.001$, and $^{****}p < 0.0001$)[41].

Results

Retinal morphology

Fundus imaging and OCT are commonly used to evaluate retinal morphology in mice. In WT mice, fundus photography revealed distinctly retinal arteries and veins, along with uniform retinal pigmentation. Meanwhile, OCT images displayed distinguishable retinal layers, particularly the inner and outer segments of photoreceptor cells and the retinal pigment epithelium (RPE) (Fig. 1A). In Kv8.2 KO mice, retinal arteries and veins were narrowed, and retinal pigmentation was normal. The inner and outer segments of photoreceptor cells and the RPE remained clearly visible in Kv8.2 KO mice. However, the thickness of the retina and outer nuclear layer (ONL) was significantly reduced in Kv8.2 KO mice compared to WT mice (Figs. 1C, S1A,B). In rd10 mice, fundus photography showed retinal vascular atrophy, along with widespread white dot-like pigmentation changes across the retina. OCT images revealed that the inner and outer segments of photoreceptor cells and the RPE became indistinguishable, suggesting significant photoreceptor cell degeneration (Figs. 1E, S1C,D). For mice with the same genetic background, there were no significant differences in retinal morphology among the three different anesthesia groups (Fig. 1B,D,F).
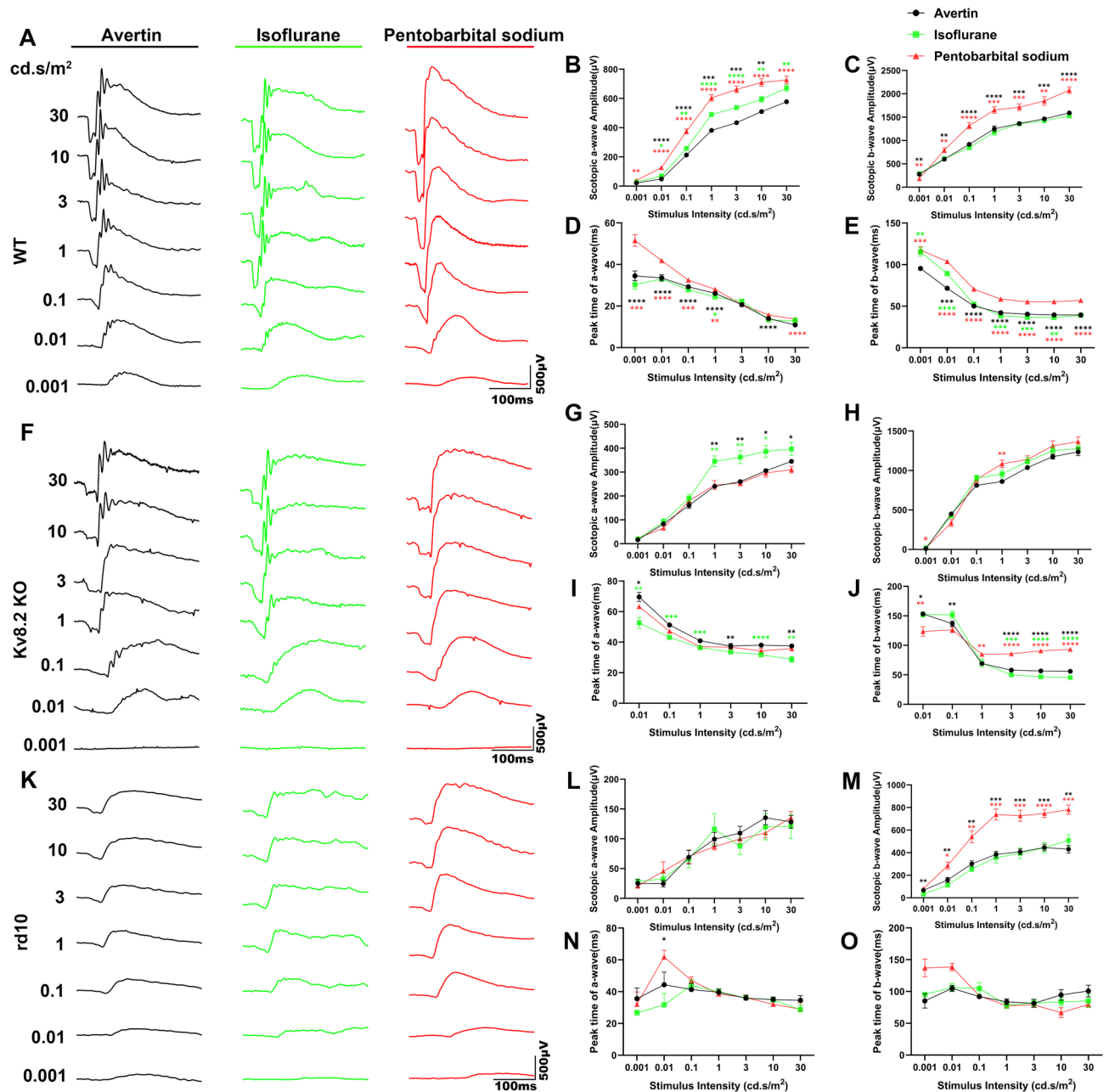
Scotopic ERG

Scotopic ERG recordings primarily reflect the electrical activity of rod cells under light stimulation. In this study, ERG recordings were conducted under dim infrared light (> 640 nm) because rod cells are insensitive to light with wavelengths greater than 640 nm.

In WT mice, the amplitudes of negative a-wave and subsequent positive b-wave increased gradually with increasing light stimulus intensity (Fig. 2A). There were significant differences in a-wave amplitudes among the three groups (Fig. 2B). The b-wave amplitudes were highest in the pentobarbital sodium group, while there were no differences between the isoflurane and avertin groups (Fig. 2C). The peak times of a-wave and b-wave were delayed in the pentobarbital sodium group compared with the other groups (Fig. 2D,E). In Kv8.2 KO mice, the a-wave amplitude was highest in the isoflurane group, while there were no significant differences between the pentobarbital sodium and avertin groups (Fig. 2F,G). However, there were no significant differences in the b-wave amplitudes among the three groups (Fig. 2F,H). The a-wave peak time was significantly shorter in the isoflurane group, with no significant differences between the pentobarbital sodium and avertin groups (Fig. 2I). The b-wave peak time was delayed from the stimulus intensity of 1 to 30 cd s/m^2 in the pentobarbital sodium group (Fig. 2J). In rd10 mice, there were no significant differences in a-wave amplitude; however, the b-wave
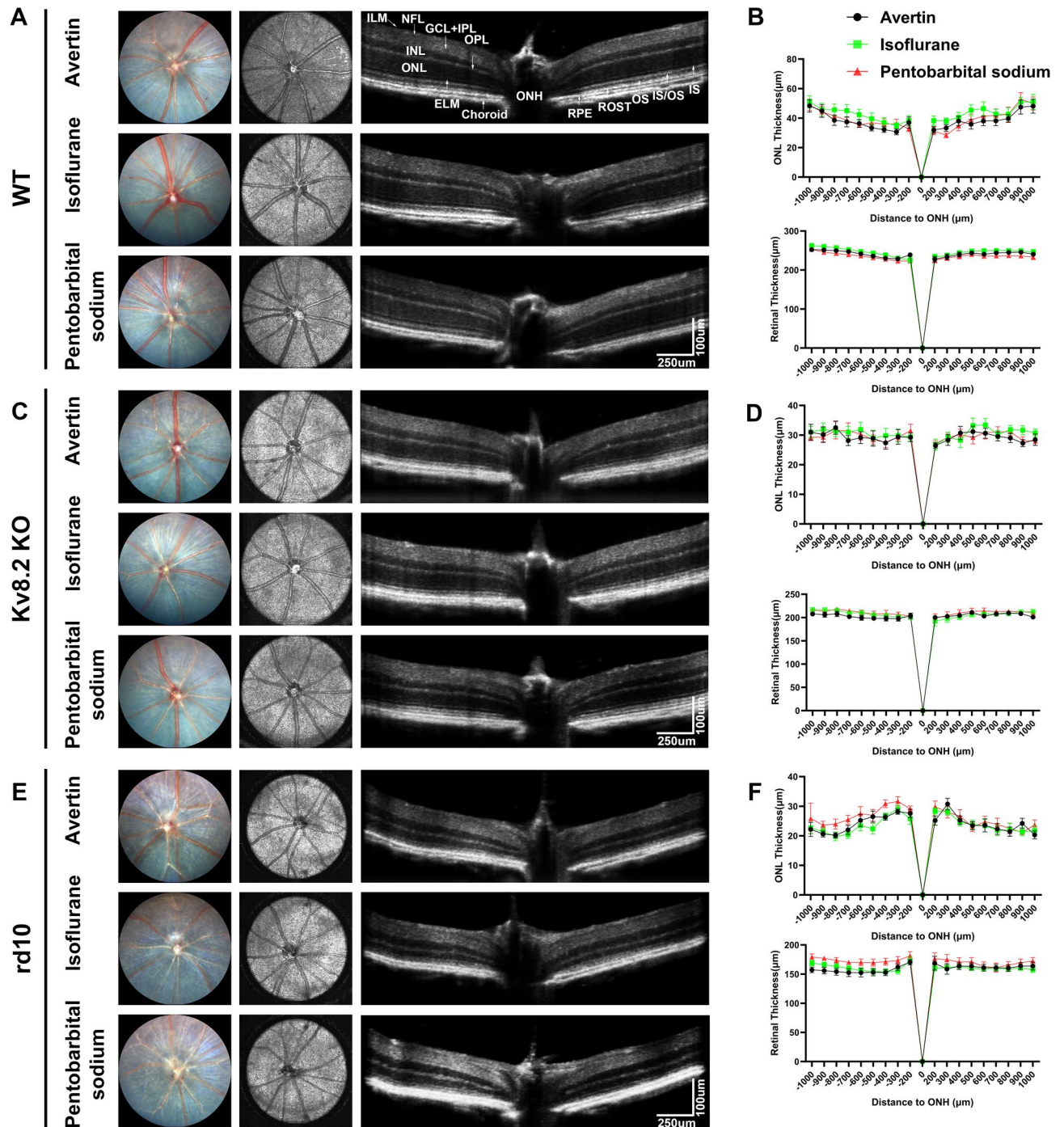
Fig. 1. Fundus images and OCT. (**A**) The left and right columns displayed fundus images and OCT of WT mice, respectively. The center column showed the optic nerve position in the process of OCT acquisition. (**B**) ONL and retina thickness measurement in WT mice. (**C**) Fundus images and OCT of Kv8.2 KO mice. (**D**) ONL and retina thickness measurement in Kv8.2 KO mice. E, Fundus images and OCT of rd10 mice. F, ONL and retina thickness measurement in rd10 mice. OCT images, the left side corresponding to the lower visual field. *OCT* optical coherence tomography; *WT* wild-type; *KO* knockout; *ILM* inner limiting membrane; *NFL* nerve fiber layer; *GCL* ganglion cell layer; *IPL* inner plexiform layer; *INL* inner nuclear layer; *OPL* outer plexiform layer; *ONL* outer nuclear layer; *OLM* outer limiting membrane; *IS* inner segments; *OS* outer segments; *IS/OS*, inner segment/outer segment complex; *ROST* rod outer segment tips; RPE, retinal pigmented epithelium.
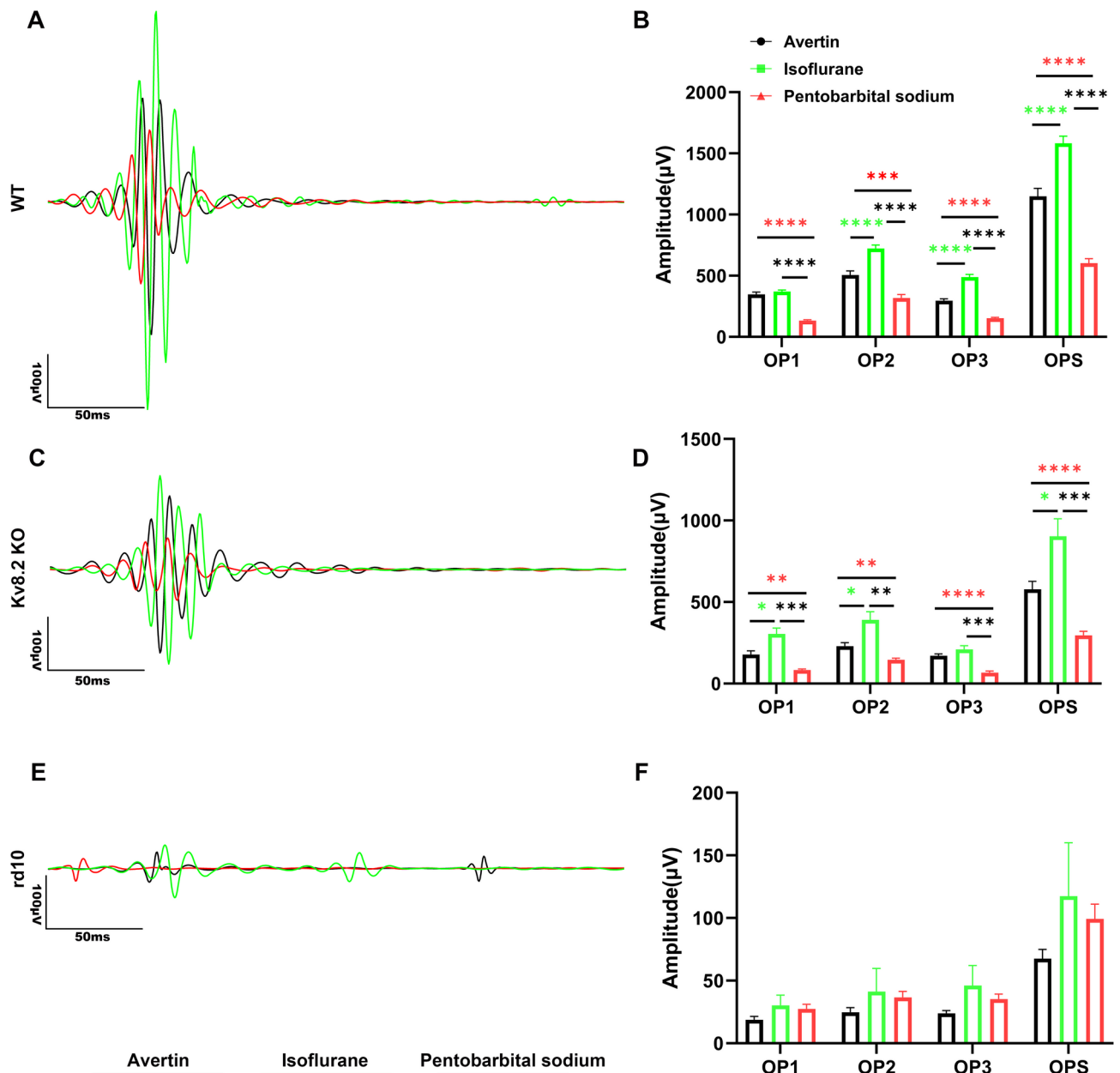
Fig. 2. Scotopic ERG in mice. (**A**, **F**, **K**) Representative waveforms of scotopic responses at different stimulus intensities in WT, Kv8.2 KO, and rd10 mice, respectively. (**B**, **G**, **L**) Quantification of the amplitude of scotopic a-waves in different mice. (**C**, **H**, **M**) Quantification of the amplitude of scotopic b-waves in different mice. (**D**, **E**, **I**, **J**, **N**, **O**) Quantification of the peak time of scotopic a-waves and b-waves in different mice, respectively. Black: Avertin group, Green: Isoflurane group, Red: Pentobarbital sodium group. Results are presented as mean ± SE; WT, n = 9–11 animals (17–22 eyes per group); KO, n = 6–9 animals (11–18 eyes per group); rd10, n = 4–5 animals (8–10 eyes per group); $^*p < 0.05$, $^{**}p < 0.01$, $^{***}p < 0.001$, $^{****}p < 0.0001$; $^*p$ (Red) represents comparisons between avertin and pentobarbital sodium groups; $^*p$ (Green), isoflurane and avertin groups; $^*p$ (Black), pentobarbital sodium and isoflurane groups.

amplitude was significantly higher in the pentobarbital sodium group (Fig. 2K–M). No significant differences in a- and b-wave peak times in rd10 mice were observed among the three groups (Fig. 2N,O). We also compared the scotopic a-wave and b-wave amplitudes among the three types of mice under the same anesthetic (Fig. S2). It was observed that the amplitudes of a-wave and b-wave progressively decreased from WT to Kv8.2 KO, and then to rd10 mice under avertin (Fig. S2A,B), isoflurane (Fig. S2C,D), and pentobarbital sodium (Fig. S2E,F) anesthesia.

Oscillatory potentials

OPs, appearing as triphasic spikes on the positive b-wave, were noticeable and became more pronounced with increasing stimulus intensity (Fig. 2). As shown in Fig. 3, we recorded the OPs at stimulus intensities of 3 cd s/m². In WT mice, three to five OPs peaks were observed (Fig. 3A), with the highest amplitude in the isoflurane group and the lowest in the pentobarbital sodium group (Fig. 3B). In Kv8.2 KO mice, there was a mild reduction in OPs (Fig. 3C), with the highest amplitude in the isoflurane group and the lowest in the pentobarbital sodium group (Fig. 3D). In rd10 mice, the OP amplitudes were very low, and no significant differences were observed among the three groups (Fig. 3F). The scotopic OP amplitudes were also compared among the three types of mice under the same anesthetic (Fig. S3). It was observed that the OPs amplitudes consistently decreased sequentially in the WT, Kv8.2 KO, and rd10 mice under avertin (Fig. S3A), isoflurane (Fig. S3B), and pentobarbital sodium (Fig. S3C) anesthesia.
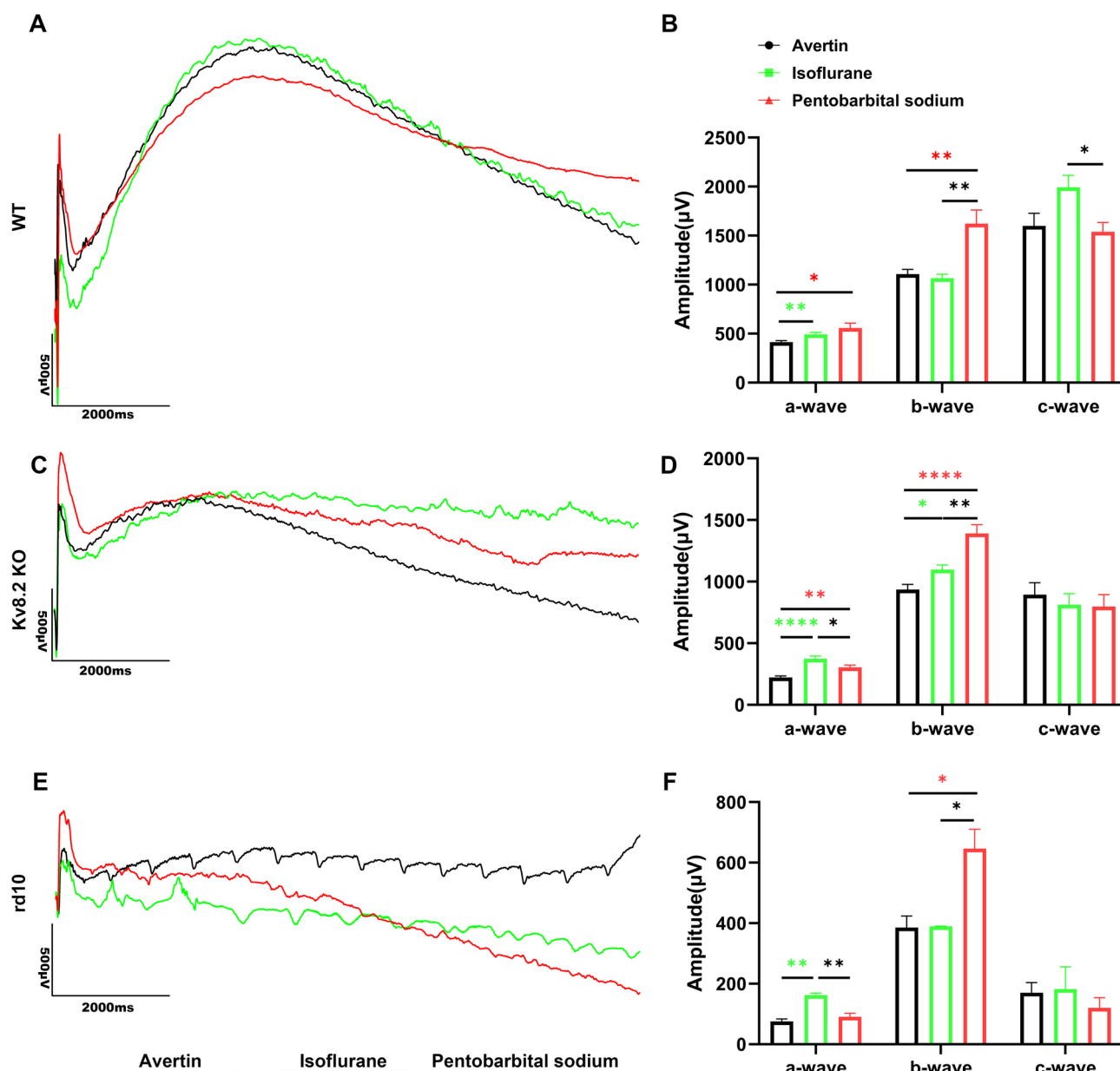

Fig. 3. Scotopic OPs in mice. (**A, C, E**) Representative waveforms of scotopic OPs at a stimulus intensity of 3 cd s/m² in WT, Kv8.2 KO, and rd10 mice, respectively. (**B, D, F**) Quantification of the amplitude of scotopic OPs in different mice. Black: Avertin group, Green: Isoflurane group, Red: Pentobarbital sodium group. Results are presented as mean ± SE; WT, n = 9–11 animals (17–22 eyes per group); KO, n = 6–9 animals (11–18 eyes per group); rd10, n = 3–6 animals (4–12 eyes per group). $^*p < 0.05$, $^{**}p < 0.01$, $^{***}p < 0.001$, $^{****}p < 0.0001$.

C-wave

In WT mice in this study, a prominent c-wave closely followed the b-wave (Fig. 4A). Figure 4B shows that the c-wave amplitude of WT mice was higher in the isoflurane group than in the other two groups. In Kv8.2 KO mice, the c-wave amplitude was lower than the b-wave amplitude, while the amplitude of c-waves was comparable among the three groups (Fig. 4C,D). In rd10 mice, a typical c-wave was barely recordable (Fig. 4E,F). Differences in c-wave amplitude among the three types of mice were also significant under the same anesthetic (Fig. S4).
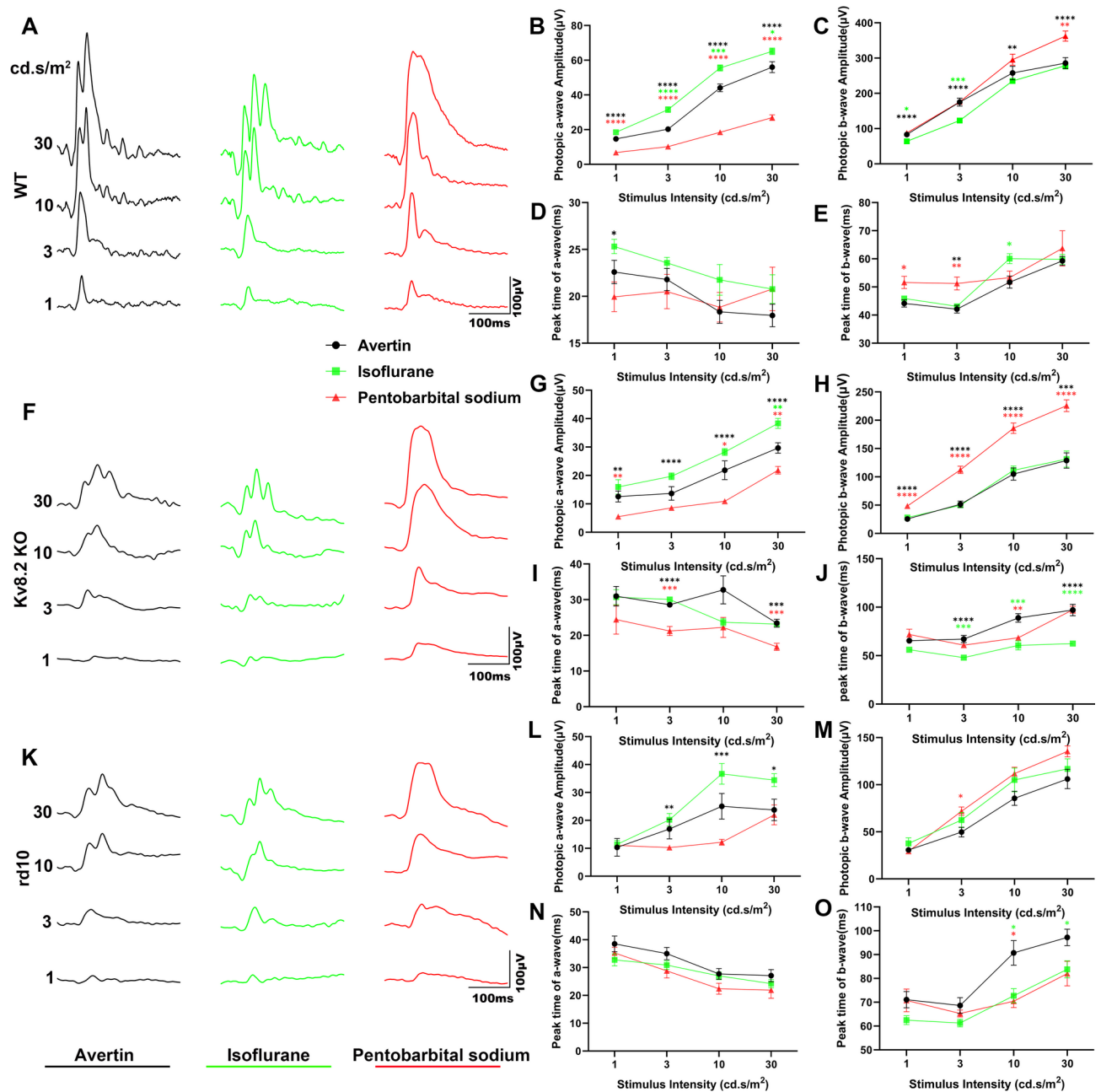
Photopic ERG

Photopic ERG a-waves, with lower amplitudes and less distinct waveforms compared with scotopic ERG, were recorded in three types of mice (Fig. 5A,B,F,G,K,L). The amplitudes of a-waves from high to low were as follows: isoflurane, avertin, and pentobarbital sodium group (Fig. 5B,G,L). Additionally, OPs were observed in b-waves at higher stimulus intensities in the isoflurane and avertin groups but not in the pentobarbital group (Fig. 5A,F,K). The b-wave amplitudes of WT mice were highest in the pentobarbital sodium group at the light intensities of 10 and 30 cd s/m^2 (Fig. 5C). In Kv8.2 KO mice, the b-wave amplitudes were highest in the pentobarbital

Fig. 4. Scotopic c-waves in mice. (**A**, **C**, **E**) Representative waveforms of c-waves were recorded at a stimulus intensity of 150 cd/m^2 in WT, KO, and rd10 mice, respectively. (**B**, **D**, **F**) Quantification of the amplitude of c-waves in different mice. Black: Avertin group, Green: Isoflurane group, Red: Pentobarbital sodium group. Results are presented as mean ± SE; WT, n = 9–11 animals (17–22 eyes per group); KO, n = 6–9 animals (11–18 eyes per group); rd10, n = 3–6 animals (4–12 eyes per group). $^*p < 0.05$, $^{**}p < 0.01$, $^{***}p < 0.001$, $^{****}p < 0.0001$.
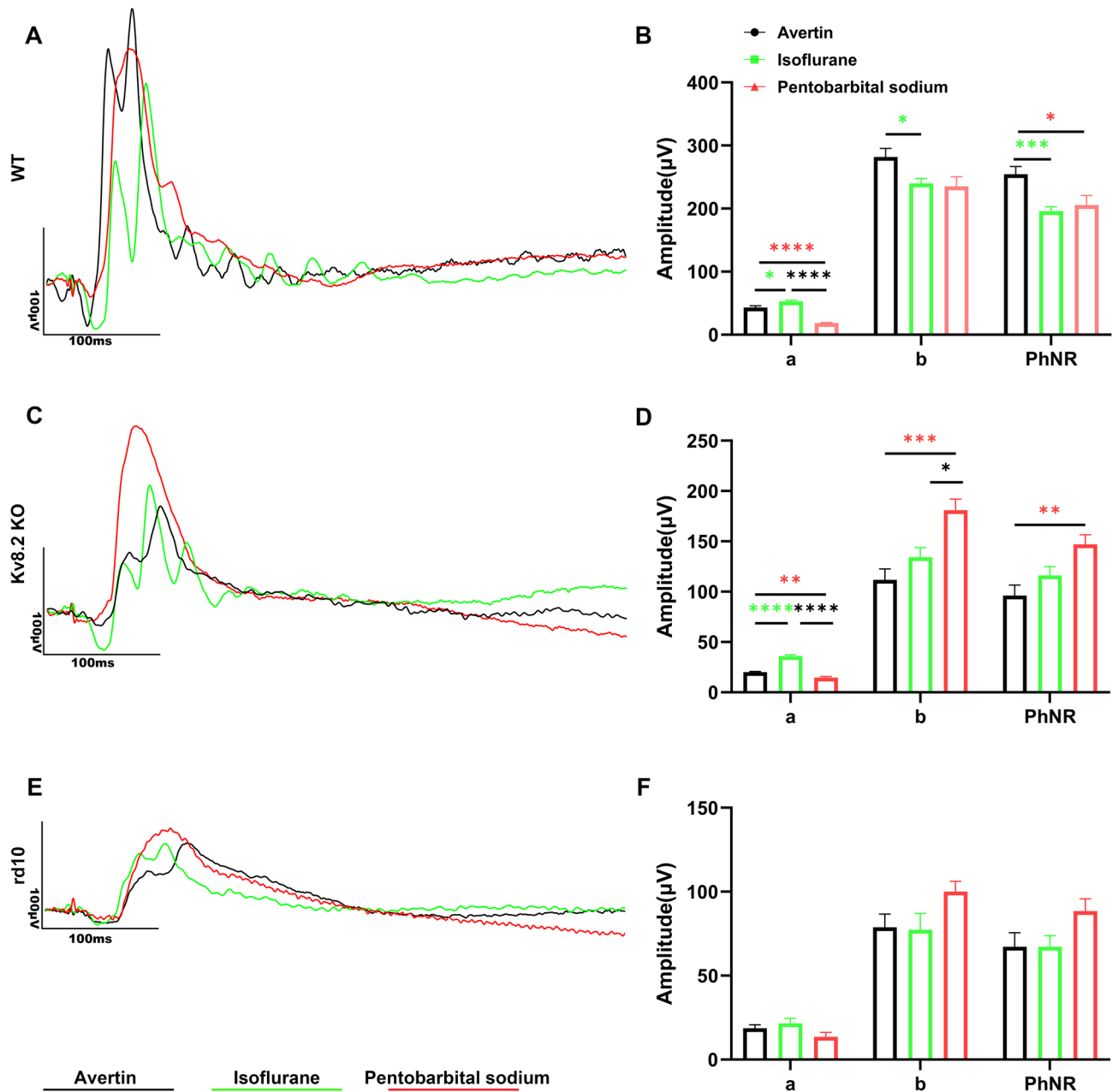
Fig. 5. Photopic ERG in mice. (**A**, **F**, **K**) Representative waveforms of photopic responses in WT, Kv8.2 KO, and rd10 mice, respectively. (**B**, **G**, **L**) Quantification of the amplitude of photopic a-waves in different mice. (**C**, **H**, **M**) Quantification of the amplitude of photopic b-waves in different mice. (**D**, **E**, **I**, **J**, **N**, **O**) Quantification of the peak time of photopic a-waves and b-waves in different mice, respectively. Black: Avertin group, Green: Isoflurane group, Red: Pentobarbital sodium group. Results are presented as mean ± SE; WT, n = 9–11 animals (17–22 eyes per group); KO, n = 6–9 animals (11–17 eyes per group); rd10, n = 4–6 animals (8–11 eyes per group); $^*p < 0.05$, $^{**}p < 0.01$, $^{***}p < 0.001$, $^{****}p < 0.0001$; $^*p$ (Red) represents comparisons between avertin and pentobarbital sodium groups; $^*p$ (Green), isoflurane and avertin groups; $^*p$ (Black), pentobarbital sodium and isoflurane groups.

sodium group, with no significant differences between the other two groups (Fig. 5H). Furthermore, there were no significant differences in b-wave amplitudes of rd10 mice among the three anesthesia groups (Fig. 5M). Additionally, the a-wave and b-wave amplitudes of WT mice were highest under all three anesthetics (Fig. S5A,C,E). However, the b-wave amplitudes of Kv8.2 KO and rd10 mice showed significant differences only when anesthetized with pentobarbital sodium (Fig. S5B,D,F). In terms of peak time, there were no consistent and meaningful differences among the three anesthetic groups (Fig. 5D,E,I,J,N,O).

Fig. 6. PhNR in Mice. (**A**, **C**, **E**) Representative waveforms of PhNR at a stimulus intensity of 20 cd s/m^2 on a green background of 40 cd/m^2 in WT, Kv8.2 KO, and rd10 mice, respectively. (**B**, **D**, **F**) Quantification of the amplitude of C-waves in different mice. Black: Avertin group, Green: Isoflurane group, Red: Pentobarbital sodium group. Results are presented as mean ± SE; WT, n = 9–11 animals (17–22 eyes per group); KO, n = 6–9 animals (11–17 eyes per group); rd10, n = 4–5 animals (4–9 eyes per group). $^*p < 0.05$, $^{**}p < 0.01$, $^{***}p < 0.001$, $^{****}p < 0.0001$.

PhNR

PhNR, including a- and b-wave, were recorded at a stimulus intensity of 20 cd s/m^2 on a green background of 40 cd/m^2. A typical PhNR, as a negative wave following the b-wave, was only recorded in WT mice (Fig. 6A,C,E). In WT mice, double-peaked b-waves were observed in the avertin and isoflurane groups but not in the pentobarbital sodium group (Fig. 6A). The PhNR amplitude was highest in the avertin group, the a-wave amplitude was highest in the isoflurane group, and the b-wave amplitude was highest in the avertin group (Fig. 6B). In Kv8.2 KO mice, double or triphasic b-waves were observed in the avertin and isoflurane groups but not in the pentobarbital sodium group (Fig. 6C). The PhNR amplitude was highest in the pentobarbital sodium group, the a-wave amplitude was highest in the isoflurane group, and the b-wave amplitude was highest in the pentobarbital sodium group (Fig. 6D). In rd10 mice, double-peaked b-waves were observed in the avertin and isoflurane groups but not in the pentobarbital sodium group (Fig. 6E). There were no significant differences

among the three groups (Fig. 6F). The PhNR and b-wave amplitudes in WT mice were highest compared with the Kv8.2 KO and rd10 mice under the three anesthetic conditions (Fig. S6).

Additionally, we recorded the anesthesia induction time for the three mouse models. The average time to loss of righting reflex was 1.48 ± 0.86 min for Avertin, 7.49 ± 2.78 min for pentobarbital sodium, and 0.78 ± 0.25 min for isoflurane induction. The anesthesia durations were 56.58 ± 12.83 min for Avertin and 48.94 ± 4.53 min for pentobarbital sodium. Isoflurane, administered via continuous inhalation, provided sufficient depth and duration to complete the entire ERG procedure. After cessation of isoflurane, mice regained spontaneous movement after 3.23 ± 0.92 min.

Discussion

This study systematically evaluated the effects of three different anesthetics—avertin, isoflurane and pentobarbital sodium—on ERG recordings in WT, Kv8.2 KO and rd10 mice. The results indicated that these anesthetics significantly influenced ERG recordings without inducing acute retinal damage. Specifically, under the three anesthetic conditions, no significant differences were observed in fundus images and OCT among mice with the same genetic background. Interestingly, in terms of ERG recordings, pentobarbital sodium significantly suppressed OPs in WT and Kv8.2 KO mice. Inconsistently, pentobarbital sodium resulted in higher b-waves, which included OPs waves in both scotopic and photopic ERG. Additionally, scotopic ERG showed higher a-waves, whereas photopic ERG displayed lower a-waves in the pentobarbital sodium group. Isoflurane resulted in higher scotopic OPs, photopic a-waves, and c-waves in WT mice. Avertin showed lower a-waves in scotopic ERG and higher PhNR waves in WT mice.

Pentobarbital sodium, a fast-acting central nervous system depressant, induces loss of consciousness and cardiovascular depression through its action on GABA receptors[35]. Its primary adverse effects include respiratory and cardiovascular depression, such as reduced blood pressure[42], which may lead to ischemia in the inner retinal layers, contributing to the suppression of OPs[43]. Pentobarbital sodium enhances GABA's inhibitory action by prolonging the opening of chloride ion channels[44]. GABA, the main inhibitory neurotransmitter in the retina, is used by various retinal cells, including horizontal and amacrine cells, which may explain the suppression of OPs[45]. Furthermore, pentobarbital sodium inhibits Ca^{2+} influx through interaction with nicotinic acetylcholine receptors[46]. As retinal photoreceptors rely on Ca^{2+} for glutamate release, this inhibition likely explains the increased b-wave amplitudes in scotopic and photopic ERG[47]. Previous studies have demonstrated "rod saturation" during pentobarbital sodium anesthesia, further supporting its impact on retinal function[48].

Previous studies have reported that isoflurane has inconsistent effects on ERG. Gerritsen et al. showed that there were no significant differences in the ERG recordings of rabbits anesthetized with isoflurane or ether[49]. Van Norren et al. also found that isoflurane had no obvious effects on the ERG waveform[50]. However, Raitta et al. demonstrated that the amplitudes of the a-wave and b-wave were reduced in patients under isoflurane anesthesia, while peak time remained unchanged[51]. In this study, there was no significant reduction in scotopic a-waves in the three mouse strains under isoflurane anesthesia. Specially, a-wave amplitudes in Kv8.2 KO mice were higher in the isoflurane group compared with the other two groups, while the b-wave was comparable to that under avertin and weaker than with pentobarbital sodium.

OPs are believed to reflect feedback synaptic circuits originating from the inner nuclear layer, where GABA and glycine serve as inhibitory neurotransmitters. The application of these substances selectively abolished retinal oscillatory potentials in mudpuppies[52]. However, in this study, the waveform and amplitude of retinal oscillatory potentials under isoflurane anesthesia were not significantly abolished. Volatile anesthetics can inhibit GABA processing and cause its accumulation at synaptic sites, making OPs particularly sensitive to anesthetic agents[53]. This was corroborated in this study, where isoflurane led to significantly heightened OPs. In rhesus monkeys, ERG showed that all volatile anesthetics delayed dark adaptation[54]. Although we did not assess dark adaptation in this study, isoflurane shortened the peak times of scotopic a-waves and b-waves in WT and Kv8.2 KO mice, consistent with previous studies in mice[55].

Avertin has been widely used as a general anesthetic for experimental animals, particularly rodents[37], due to its ease of preparation and administration, as well as its broad therapeutic window compared to its lethal dose[33]. It is known to rapidly induce short-term anesthesia with prompt recovery. However, the primary adverse effect of avertin is peritonitis, which is linked to the toxicity of its metabolite, dibromoaldehyde. As a result, repeated injections of avertin can lead to a high mortality rate[56]. Avertin is also known to raise blood glucose levels, which can increase the b-wave of the ERG[57]. Studies involving the elevated plus maze (EPM) in rats found that avertin was unsuitable for surgical anesthesia prior to behavioral analysis in the EPM, as it could cause both anxious and anti-anxiety behaviors, complicating results in this commonly used visual research test[58]. The choice of anesthetic significantly impacts respiratory rate, with 1.5% isoflurane resulting in the lowest respiratory rate and avertin producing the highest[59]. Among the three anesthetic agents used in this study, we observed that animals anesthetized with avertin were more prone to irregular interference waves, which may be attributed to the higher respiratory rate induced by avertin anesthesia.

Neurotransmitter-gated ion channels, particularly GABA and glutamate receptors, are regulated by most anesthetics at both synaptic and extrasynaptic sites[60]. $GABA_A$ receptors are key targets for anesthetics such as pentobarbital sodium, avertin, and isoflurane[61]. Most inhalational anesthetics, including isoflurane, enhance $GABA_A$ receptor activity while reducing glutamate release, thereby increasing channel opening[62]. Therefore, the effects of anesthetics on ERG should be considered. Given these effects, it is essential to account for the impact of anesthetics on ERG measurements.

In this study, pentobarbital sodium significantly suppressed Ops in WT and Kv8.2 mice, making it unsuitable for recording inner retinal layer function. OPs have important clinical value in cases of diabetic retinopathy and other ischemic retinal diseases[63,64], so pentobarbital sodium should be carefully considered in such studies. Pentobarbital sodium also caused a marked reduction in the amplitudes of the photopic a-wave, which reflects

retina cone function. Isoflurane and Avertin had more moderate effects, potentially making them more suitable for various ERG recordings. However, considering that Avertin is associated with more severe side effects, isoflurane is undoubtedly the best choice, despite the need for a slightly more expensive gas anesthesia apparatus. The results of this study highlight the importance of selecting anesthetics in retinal research and offer valuable insights for improving the accuracy of ERG recordings.

Anesthetics can increase blood glucose levels, thereby enhancing retinal sensitivity[65]. Avertin and pentobarbital sodium have been shown to significantly elevate blood glucose in wild-type mice, potentially affecting ERG amplitudes[57], while isoflurane, though milder in this regard, has been reported to impair insulin secretion and aggravate both peripheral and central insulin resistance in type 2 diabetic mice[66,67]. Therefore, the choice of anesthetic may require greater caution when recording ERG in animal models of diabetic retinopathy. However, there are few studies comparing the effects of different anesthetics on ERG recordings in animal models of diabetic retinopathy. Hasegawa et al. compared pentobarbital sodium and a medetomidine-midazolam-butorphanol (MMB) combination in Spontaneously Diabetic Torii (SDT) fatty rats and found that MMB allowed for better visualization of oscillatory potentials (OPs), suggesting its potential superiority for evaluating inner retinal function in diabetic animals[68]. Miwa et al. further demonstrated that MMB significantly enhanced OPs in healthy mice, supporting its suitability for inner retinal assessments[69]. In contrast, Connell et al. reported that in STZ-induced diabetic rats, both medetomidine and xylazine failed to provide sufficient anesthetic depth, whereas pentobarbital sodium yielded more reliable ERG recordings[70]. In summary, while medetomidine and its combinations are increasingly used in rodent ERG studies, particularly in rats, their application in diabetic mouse models is not well established. Given the relatively mild metabolic impact and stable ERG signals observed with isoflurane in our study, it may be a more appropriate choice for ERG testing in diabetic mouse models. Further research comparing anesthetic protocols under pathological conditions is warranted to refine best practices for retinal electrophysiological assessments.

Nevertheless, there are certain limitations to this study that need to be addressed. For instance, we were unable to obtain ketamine and xylazine for comparison, limiting our findings. This limitation further underscores the importance of comparing these three easily prepared and administered anesthetics simultaneously. Including more recordings from ERG waveforms, visual evoked potentials (VEP), and using mice of different ages and sexes would provide better guidance for selecting anesthetics in ERG recordings. The potential influence of sex on anesthetic response and ERG outcomes was not addressed in this study. Previous research suggests that hormonal and metabolic differences between male and female mice may affect both anesthetic pharmacodynamics and retinal function[71,72]. Therefore, future studies should include both sexes to evaluate possible sex-specific effects on ERG recordings. Additionally, variability in anesthetic administration may introduce bias into the results. Future research should focus on establishing standardized anesthetic protocols and investigating the long-term effects of these anesthetics on retinal health and function. Expanding the study with a larger sample size and additional mouse strains, while optimizing statistical analysis methods by incorporating covariates such as weight and sex to minimize confounding factors, could provide a more comprehensive understanding of how anesthetics affect retinal electrophysiology.

Data availability
All relevant data supporting the findings of this study are provided in this paper. Access to raw data is available from the corresponding author upon reasonable request.

References
1. Robson, A. G. et al. ISCEV Standard for full-field clinical electroretinography (2022 update). *Doc. Ophthalmol.* **144**, 165–177 (2022).
2. Tonade, D. & Kern, T. S. Photoreceptor cells and RPE contribute to the development of diabetic retinopathy. *Prog. Retin. Eye Res.* **83**, 100919 (2021).
3. Wang, Y., Punzo, C., Ash, J. D. & Lobanova, E. S. Tsc2 knockout counteracts ubiquitin-proteasome system insufficiency and delays photoreceptor loss in retinitis pigmentosa. *Proc. Natl. Acad. Sci. U. S. A.* **119**, e2118479119 (2022).
4. Wang, S. et al. CXCL1-CXCR2 signalling mediates hypertensive retinopathy by inducing macrophage infiltration. *Redox Biol.* **56**, 102438 (2022).
5. Okimura, K., Nakane, Y., Nishiwaki-Ohkawa, T. & Yoshimura, T. Photoperiodic regulation of dopamine signaling regulates seasonal changes in retinal photosensitivity in mice. *Sci. Rep.* **11**, 1843 (2021).
6. Kong, Y. et al. HIF2α activation and mitochondrial deficit due to iron chelation cause retinal atrophy. *EMBO Mol. Med.* **15**, e16525 (2023).
7. Casson, R. J., Chidlow, G., Crowston, J. G., Williams, P. A. & Wood, J. P. M. Retinal energy metabolism in health and glaucoma. *Prog. Retin. Eye Res.* **81**, 100881 (2021).
8. Sethna, S. et al. CIB2 regulates mTORC1 signaling and is essential for autophagy and visual function. *Nat. Commun.* **12**, 3906 (2021).
9. Hart, N. et al. The role of the voltage-gated potassium channel proteins Kv8.2 and Kv2.1 in vision and retinal disease: Insights from the study of mouse gene knock-out mutations. *eNeuro* **6**, ENEURO.032-19.2019 (2019).
10. Jiang, X. et al. Molecular, cellular and functional changes in the retinas of young adult mice lacking the voltage-gated K+ channel subunits Kv8.2 and K2.1. *Int. J. Mol. Sci.* **22**, 4877 (2021).
11. Inamdar, S. M. et al. Differential impact of Kv8.2 loss on rod and cone signaling and degeneration. *Hum. Mol. Genet.* **31**, 1035–1050 (2022).
12. Ebeling, M. C. et al. Improving retinal mitochondrial function as a treatment for age-related macular degeneration. *Redox Biol.* **34**, 101552 (2020).
13. Gorbatyuk, M. S., Starr, C. R. & Gorbatyuk, O. S. Endoplasmic reticulum stress: New insights into the pathogenesis and treatment of retinal degenerative diseases. *Prog. Retin. Eye Res.* **79**, 100860 (2020).

14. Chang, B. et al. Retinal degeneration mutants in the mouse. *Vision Res.* **42**, 517–525 (2002).
15. Mahato, B. et al. Pharmacologic fibroblast reprogramming into photoreceptors restores vision. *Nature* **581**, 83–88 (2020).
16. Hata, M. et al. Past history of obesity triggers persistent epigenetic changes in innate immunity and exacerbates neuroinflammation. *Science* **379**, 45–62 (2023).
17. Weymouth, A. & Vingrys, A. Rodent electroretinography: Methods for extraction and interpretation of rod and cone responses. *Prog. Retin. Eye Res.* **27**, 1–44 (2008).
18. Belforte, N. et al. AMPK hyperactivation promotes dendrite retraction, synaptic loss, and neuronal dysfunction in glaucoma. *Mol. Neurodegener.* **16**, 43 (2021).
19. Sachdeva, B., Sachdeva, P., Ghosh, S., Ahmad, F. & Sinha, J. K. Ketamine as a therapeutic agent in major depressive disorder and posttraumatic stress disorder: Potential medicinal and deleterious effects. *Ibrain* **9**, 90–101 (2023).
20. Cohen, S. P. et al. Consensus guidelines on the use of intravenous ketamine infusions for chronic pain from the american society of regional anesthesia and pain medicine, the american academy of pain medicine, and the American Society of Anesthesiologists. *Reg. Anesth. Pain Med.* **43**, 521–546 (2018).
21. Peltoniemi, M. A., Hagelberg, N. M., Olkkola, K. T. & Saari, T. I. Ketamine: A review of clinical pharmacokinetics and pharmacodynamics in anesthesia and pain therapy. *Clin. Pharmacokinet.* **55**, 1059–1077 (2016).
22. Telias, M. et al. Retinoic acid inhibitors mitigate vision loss in a mouse model of retinal degeneration. *Sci. Adv.* **8**, eabm4643 (2022).
23. Hanaguri, J. et al. The effect of sodium-dependent glucose cotransporter 2 inhibitor tofogliflozin on neurovascular coupling in the retina in type 2 diabetic mice. *Int. J. Mol. Sci.* **23**, 1362 (2022).
24. Gong, Y. et al. The effect of a chrysanthemum water extract in protecting the retina of mice from light damage. *BMC Complement. Med. Ther.* **22**, 224 (2022).
25. Zhang, H. et al. Electroretinogram of the cone-dominant thirteen-lined ground squirrel during euthermia and hibernation in comparison with the rod-dominant brown norway rat. *Invest. Ophthalmol. Visual Sci.* **61**, 6 (2020).
26. Victorino, D. B., Scott-McKean, J. J., Johnson, M. W. & Costa, A. C. S. Quantitative analysis of retinal structure and function in two chromosomally altered mouse models of down syndrome. *Invest. Ophthalmol. Visual Sci.* **61**, 25 (2020).
27. Zhou, Z. et al. Distinguished functions of microglia in the two stages of oxygen-induced retinopathy: A novel target in the treatment of ischemic retinopathy. *Life* **12**, 1676 (2022).
28. Zhang, Y. et al. Monocular deprivation affects visual cortex plasticity through cPKCγ-Modulated GluR1 phosphorylation in mice. *Invest. Ophthalmol. Visual Sci.* **61**, 44 (2020).
29. Moult, E. M. et al. Evaluating anesthetic protocols for functional blood flow imaging in the rat eye. *J. Biomed. Opt.* **22**, 16005 (2017).
30. Choh, V. et al. Isoflurane and ketamine:xylazine differentially affect intraocular pressure-associated scotopic threshold responses in Sprague-Dawley rats. *Doc. Ophthalmol.* **135**, 121–132 (2017).
31. Constantinides, C., Mean, R. & Janssen, B. J. Effects of Isoflurane Anesthesia on the Cardiovascular Function of the C57BL/6 Mouse. *ILAR J. Natl. Res. Counc. Inst. Lab. Anim. Resour.* **52**, e21–e31 (2011).
32. Thompson, J. S. et al. Early effects of tribromoethanol, ketamine/xylazine, pentobarbitol, and isoflurane anesthesia on hepatic and lymphoid tissue in ICR mice. *Comp. Med.* **52**, 63–67 (2002).
33. Maheras, K. J. & Gow, A. Increased anesthesia time using 2,2,2-tribromoethanol–chloral hydrate with low impact on mouse psychoacoustics. *J. Neurosci. Methods* **219**, 61–69 (2013).
34. Chaudhary, V., Hansen, R., Lindgren, H. & Fulton, A. Effects of telazol and nembutal on retinal responses. *Doc. Ophthalmol.* **107**, 45–51 (2003).
35. Mohamed, A. S. et al. Sodium pentobarbital dosages for exsanguination affect biochemical, molecular and histological measurements in rats. *Sci. Rep.* **10**, 378 (2020).
36. Xie, H. et al. Differential effects of anesthetics on resting state functional connectivity in the mouse. *J. Cereb. Blood Flow Metab.* **40**, 875–884 (2020).
37. Wang, D. et al. Avertin affects murine colitis by regulating neutrophils and macrophages. *Int. Immunopharmacol.* **80**, 106153 (2020).
38. Pachon, R. E., Scharf, B. A., Vatner, D. E. & Vatner, S. F. Best anesthetics for assessing left ventricular systolic function by echocardiography in mice. *Am. J. Physiol. Heart Circ. Physiol.* **308**, H1525–H1529 (2015).
39. Zheng, S. et al. Activation of liver X receptor protects inner retinal damage induced by N-methyl-D-aspartate. *Invest. Ophthalmol. Visual Sci.* **56**, 1168–1180 (2015).
40. Kim, K. et al. All-printed stretchable corneal sensor on soft contact lenses for noninvasive and painless ocular electrodiagnosis. *Nat. Commun.* **12**, 1544 (2021).
41. Ge, Y. et al. Key transcription factors influence the epigenetic landscape to regulate retinal cell differentiation. *Nucleic Acids Res.* **51**, 2151 (2023).
42. Hildebrandt, I. J., Su, H. & Weber, W. A. Anesthesia and other considerations for in vivo imaging of small animals. *ILAR J.* **49**, 17–26 (2008).
43. Barboni, M. T. S., Sustar Habjan, M., Petrovic Pajic, S. & Hawlina, M. Electroretinographic oscillatory potentials in Leber hereditary optic neuropathy. *Doc. Ophthalmol.* **148**, 133–143 (2024).
44. Walker, S. E. & Iazzetta, J. Compatibility and stability of pentobarbital in infusions. *Anesthesiology* **55**, 487–489 (1981).
45. Popova, E. ON-OFF interactions in the retina: Role of glycine and GABA. *Curr. Neuropharmacol.* **12**, 509–526 (2014).
46. Weber, M. et al. Intravenous anaesthetics inhibit nicotinic acetylcholine receptor-mediated currents and Ca^{2+} transients in rat intracardiac ganglion neurons. *Br. J. Pharmacol.* **144**, 98–107 (2005).
47. Rashwan, R., Hunt, D. M. & Carvalho, L. S. The role of voltage-gated ion channels in visual function and disease in mammalian photoreceptors. *Pflüg. Arch.* https://doi.org/10.1007/s00424-021-02595-2 (2021).
48. Brown, C. H. & Green, D. G. Rod saturation in b-wave of the rat electroretinogram under two different anesthetics. *Vision Res.* **24**, 87–90 (1984).
49. Gerritsen, B. G. The effect of anaesthetics on the electroretinogram and the visually evoked response in the rabbit. *Doc. Ophthalmol.* **29**, 289–330 (1971).
50. van Norren, D. & Padmos, P. Cone dark adaptation: The influence of halothane anesthesia. *Invest. Ophth. Visual.* **14**, 212–227 (1975).
51. Raitta, C., Karhunen, U., Seppälainen, A. M. & Naukkarinen, M. Changes in the electroretinogram and visual evoked potentials during general anaesthesia. *Albr. Von Graefes Arch. Fur Klin. Exp. Ophthalmol.* **211**, 139–144 (1979).
52. Wachtmeister, L. & Dowling, J. E. The oscillatory potentials of the mudpuppy retina. *Invest. Ophthalmol. Visual Sci.* **17**, 1176–1188 (1978).
53. Tashiro, C. et al. Electroretinogram as a possible monitor of anesthetic depth. *Graefe's Arch. Clin. Exp. Ophthalmol. = Albr. Von Graefes Arch. Fur Klin. Exp. Ophthalmol.* **224**, 473–476 (1986).
54. van Norren, D. & Padmos, P. Influence of anesthetics, ethyl alcohol, and Freon on dark adaptation of monkey cone ERG. *Invest. Ophthalmol. Visual Sci.* **16**, 80–83 (1977).
55. Woodward, W. R. et al. Isoflurane is an effective alternative to ketamine/xylazine/acepromazine as an anesthetic agent for the mouse electroretinogram. *Doc. Ophthalmol.* **115**, 187–201 (2007).
56. Zeller, W., Meier, G., Bürki, K. & Panoussis, B. Adverse effects of tribromoethanol as used in the production of transgenic mice. *Lab. Anim.* **32**, 407–413 (1998).

57. Brown, E. T., Umino, Y., Loi, T., Solessio, E. & Barlow, R. Anesthesia can cause sustained hyperglycemia in C57/BL6J mice. *Vis. Neurosci.* **22**, 615–618 (2005).
58. Herbst, L. S. et al. New evidence for refinement of anesthetic choice in procedures preceding the forced swimming test and the elevated plus-maze. *Behav. Brain Res.* **368**, 111897 (2019).
59. Niles, D. J., Gordon, J. W. & Fain, S. B. Effect of anesthesia on renal R2* measured by blood oxygen level-dependent MRI. *NMR Biomed.* **28**, 811–817 (2015).
60. Hemmings, H. C. et al. Emerging molecular mechanisms of general anesthetic action. *Trends Pharmacol. Sci.* **26**, 503–510 (2005).
61. Franks, N. P. & Lieb, W. R. Molecular and cellular mechanisms of general anaesthesia. *Nature* **367**, 607–614 (1994).
62. Krasowski, M. D. & Harrison, N. L. General anaesthetic actions on ligand-gated ion channels. *Cell. Mol. Life Sci. CMLS* **55**, 1278–1303 (1999).
63. Midena, E. et al. Early microvascular and oscillatory potentials changes in human diabetic retina: Amacrine cells and the intraretinal neurovascular crosstalk. *J. Clin. Med.* **10**, 4035 (2021).
64. Qu, Y., Ran, L., Wang, G., Wang, M. & Li, S. Oscillatory potential findings in patients with acute ischaemic central retinal vein occlusion. *BMJ Open Ophthalmol.* **9**, e001582 (2024).
65. Brown, E. T. et al. Anesthesia affects mouse ERG and blood glucose. *Invest. Ophthalmol. Vis. Sci.* **45**, 742–742 (2004).
66. Tanaka, K. et al. Mechanisms of impaired glucose tolerance and insulin secretion during isoflurane anesthesia. *Anesthesiology* **111**, 1044–1051 (2009).
67. Fang, X. et al. Isoflurane aggravates peripheral and central insulin resistance in high-fat diet/streptozocin-induced type 2 diabetic mice. *Brain Res.* **1727**, 146511 (2020).
68. Hasegawa, T. et al. Differences in the effects of pentobarbital anesthetic and combination of medetomidine hydrochloride, midazolam, and butorphanol tartrate anesthetic on electroretinogram in spontaneously diabetic torii fatty rats. *Biomed. Hub.* **7**, 106–114 (2022).
69. Miwa, Y., Tsubota, K. & Kurihara, T. Effect of midazolam, medetomidine, and butorphanol tartrate combination anesthetic on electroretinograms of mice. *Mol. Vis.* **25**, 645–653 (2019).
70. Connell, A. R. et al. Comparisons of α2-adrenergic agents, medetomidine and xylazine, with pentobarbital for anesthesia: Important pitfalls in diabetic and nondiabetic rats. *J. Ocul. Pharmacol. Ther.* **38**, 156–166 (2022).
71. Pleym, H., Spigset, O., Kharasch, E. D. & Dale, O. Gender differences in drug effects: Implications for anesthesiologists. *Acta Anaesthesiol. Scand.* **47**, 241–259 (2003).
72. Zambricki, E. A. & Dalecy, L. G. Rat sex differences in anesthesia. *Comp. Med.* **54**, 49–53 (2004).

Author contributions
C.Y. wrote the main manuscript text. X.W., K.Y., and Y.H. assisted with the experiments. S.L. and Y.W. provided funding, supervised the experimental process, and aided in revising the manuscript. All authors reviewed and approved the final manuscript.

Declarations

Competing interests
The authors declare no competing interests.

Additional information
Supplementary Information The online version contains supplementary material available at https://doi.org/10.1038/s41598-025-98924-x.

Correspondence and requests for materials should be addressed to S.L. or Y.W.

Reprints and permissions information is available at www.nature.com/reprints.

Publisher's note Springer Nature remains neutral with regard to jurisdictional claims in published maps and institutional affiliations.